

# Numerical vibro-acoustic analysis of gear pumps for automotive applications

**E. Mucchi, G. Dalpiaz**

University of Ferrara, Engineering Department

Via Saragat, 1, Ferrara – 44122, Italy

e-mail: [emiliano.mucchi@unife.it](mailto:emiliano.mucchi@unife.it)

## Abstract

In this work a combined model for the vibro-acoustic analysis of an external gear pump for automotive applications is presented and experimentally assessed. The model includes a lumped-parameter model, a finite-element model and a boundary-element model. The lumped-parameter (LP) model regards the interior parts of the pump (bearing blocks and gears), the finite element (FE) model regards the external parts of the pump (casing and end plates), while the boundary element (BE) model estimates the noise generation in operational conditions. Attention has been devoted to the inclusion of the oil effect inside the pump casing: the fluid-structure interaction between oil and pump casing was taken into account. The model has been assessed using experiments: the experimental accelerations and acoustic pressure measured in operational conditions have been compared with the simulated data coming from the combined LP/FE/BE model. Eventually, model results and limitations are presented.

## 1 Introduction

It is well known that in the automotive field there is an increasing demand for components producing low levels of noise and vibrations, for comfort reasons. Noise and vibration control is not an easy task, as the final comfort result depends on a number of factors. This task requires a good knowledge of the system dynamic behavior: to this end, mathematical models can be very useful tools for the identification of noise and vibration sources. Moreover, the use of mathematical models allows to predict the effects of design modifications and to reduce the number of tests required for design improvements. The mechanical system under study is an external gear pump for vehicle steering. The most usual configuration has two twin gears (see Figure 1), which are assembled by a couple of lateral floating bearing blocks that act as seals for the lateral ends. Gears and floating bearing blocks are jointly packed inside a casing that encloses all the components and defines the isolated spaces that carry the fluid from the low to the high pressure chamber. The bearing blocks act as supports for the gear shafts by means of two hydrodynamic bearings, which are hydraulically balanced in order to avoid misalignments between gear shaft and journal bearing. Power is applied to the shaft of one gear (gear 1) and transmitted to the driven gear (gear 2) through their meshing. The driving shaft is connected by an Oldham coupling with an electrical drive. This pump works with a pressure ranging from 3.5 to 100 bar and angular speed ranging from 1500 to 3400 rpm. The authors have already developed some research activities about the vibration modeling of the moving components of gear pumps by means of a lumped-parameter (LP) models, as well as the experimental assessment [1][2][3]. In this work a combined lumped-parameter finite-element boundary-element model of an external gear pump for automotive applications is presented and experimentally assessed.

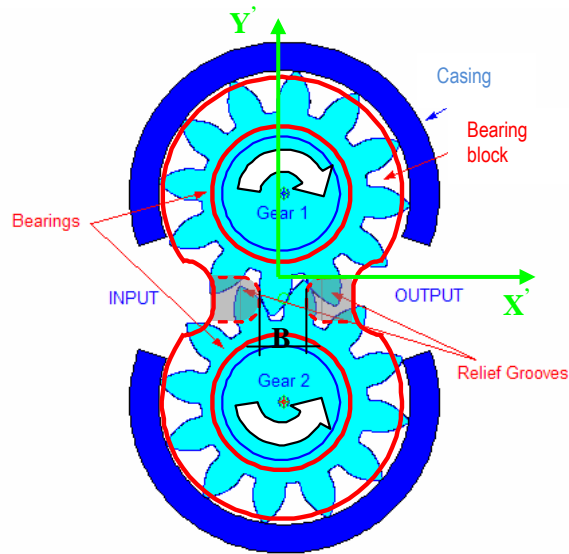


Figure 1: Schematic of the gear pump and reference frame

## 2 Method

The combined model developed in this research integrates a lumped-parameter model, a finite-element model and a boundary-element model of a gear pump. The model aims at evaluating the acceleration on the exterior parts of the gear pump (external surface of the casing, flange, cover) as well as the acoustic pressure during operational conditions. The used methodology is as follows. The lumped-parameter (LP) model of the moving components gives as output the dynamic forces and torques acting on the gears; in particular, the forces exchanged between the gears and the casing are the pressure forces and bearing reactions. These are the forces exciting the casing vibrations. Then, a finite-element (FE) model of the pump casing (also including the experimental apparatus) was developed and used in order to estimate the casing vibrations caused by the exciting forces applied by the gears and obtained by the LP model. Finally, the casing vibrations are used as input data in an indirect boundary element (BE) model for the estimation of the acoustic pressure in different operational conditions. In this sense the model is globally a combined LP/FE/BE model. For the development of the combined model it is assumed that the casing vibration produces negligible influences on the moving part dynamic behaviour. The presented model has been experimentally assessed by a number of experiments: modal analysis, frequency response function measurements, acceleration, force and acoustic pressure measurements. Hereafter, an overview of the three models and the relative validation procedures are shown.

### 2.1 Lumped parameter model of the rotating components

A non-linear lumped-parameter kineto-elastodynamic model was built in order to evaluate the dynamic behaviour of the internal components of the gear pump. The model takes into account only transversal plane dynamics; this assumption is acceptable because model regards spur gears. The model has six degrees of freedom. For each gear, degrees of freedom are the displacements along directions  $X'$  and  $Y'$  shown in Figure 1 and the angular displacement. The model includes the main important phenomena involved in the pump operation as time-varying oil pressure distribution on gears [4][5], time-varying meshing stiffness and hydrodynamic journal bearing reactions [6]. The meshing phenomena have been

widely developed; in fact, this type of gears works at low loads and consequently the effects of tooth profile errors and tooth separation could not be ignored. The model takes into account the parametric excitations due to the time-varying meshing stiffness and the tooth profile errors (obtained by a metrological analysis); the effects of the backlash between meshing teeth, the lubricant squeeze and the possibility of tooth contact on both lines of action were also included in the model. The oil pressure distribution on gears is also time-varying: it is instantaneously computed and the resultant force and torque are obtained taking into account the case wear as well as the displacement of the lateral floating bearing block. The non-linear behaviour of the hydrodynamic journal bearings is also included, as well as the torsional stiffness and damping of the driving shaft. As a consequence, the model is highly non-linear. The equations of motion give the dynamic equilibrium among the pressure forces and torques on the gears, the meshing forces, the driving external torque, the bearing reactions and the gear inertia forces and torques. The complete formulation can be found in [1][2][3]. Experimental tests were carried out on a test bench (Figure 2a) available at the company site. The pump under testing is fastened on an ergal plate that also provides proper connections to low and high pressure oil pipes; moreover the plate is equipped with four high impedance quartz-based triaxial force sensors. The pump is driven by an electrical motor equipped with inverter; the plate has a hole for the driving shaft. The assessment of the LP model was presented in [7] where the comparison between simulations and experimental results concerning forces and moments has been presented. In particular a specific validation procedure has been developed “ad hoc” for the pump under study in order to assess the dynamic model because it has not been possible to directly obtain vibration data concerning rotating components.

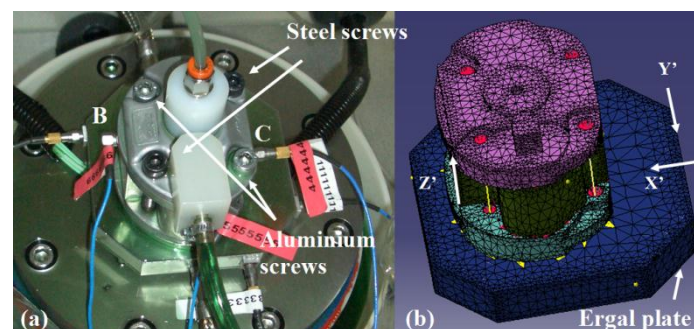


Figure 2: (a) Pump in the test bench with transducers and (b) relative FE model with reference frame  $X'Y'Z'$

## 2.2 Finite element model of the casing

The structural FE model not only regards the gear pump, but also the plate to which the pump is fastened during the experimental tests. In fact the model must be validated using experiments and therefore it has been modelled the same apparatus used for the experimental measurements, i.e. the pump, the ergal plate and the four force sensors supporting the plate as shown in Figure 2b. Obviously, once the model has been assessed, it should be possible to model the real boundary conditions as in the actual location in a vehicle. It can be noted that the test bench used in the validation of the LP/FE model is the same test bench used for the validation of the LP model (Figure 2a). In more details, the structural FE model includes the casing, the two end-plates (the lower one is indicated as flange and the upper one as cover), as well as the ergal plate to which the pump is fastened on the test bench and the four force sensors supporting the plate. The casing and the two end-plates are meshed using tetrahedral elements. In the actual pump, the three components are fastened together by means of two steel screws as shown in Figure 2a. The two screws, with proper tightening torque, guarantee the connection between the casing and the end-plates. The two screws are modelled as beam elements having the same inertia properties of the actual screws joined to the surrounding mesh of the end-plates by means of interpolation spiders (Figure 3a). The screw tightening torque is not applied to the screws in the model because it represents a static torque and therefore it gives

no contribution in a dynamic analysis. Moreover, the tightening torque produces the effect of joining the casing surface to the end-plate surfaces. Therefore, in order to model this effect, rigid spider connections are used to connect the casing surface with the end-plate surfaces as shown in Figure 3a. Furthermore, the presence of bearing blocks, oil, gears and relief valve is taken into account. Each of these components is modelled by means of a concentrated mass and an inertia momentum located in its centre of mass and connected to the surrounding mesh by means of interpolation spiders. The ergal plate of the test bench is modelled using tetrahedral elements. The ergal plate is connected to the pump by means of two aluminium screws (Figure 2a). These screws are modelled using beam elements - in the same way as for the steel screws - and are connected to the ergal plate and to the pump by means of interpolation spiders (Figure 3a). Moreover, rigid spiders are used between the end-plate lower surface and the ergal plate surface for modelling the connection between the two surfaces and in order to avoid penetration between the surfaces themselves. The ergal plate is connected to ground by four triaxial force sensors located under the ergal plate. These sensors are modelled by means of spring elements having the nominal stiffness of each sensor.

Experimental tests have been carried out in order to validate the structural FE model. In particular, frequency response function (FRF) measurements have been acquired in the pump fastened to the test bench exciting point C in direction X' (Figure 3b) by an hammer and measuring the acceleration response along the same direction by an accelerometer located in point B (Figure 3b). The FRF test has been performed in two different conditions: without oil inside the pump and with the presence of oil at 23 bar. In this second test, the 23 bar pressure has been obtained by an external equipment. Figure 4 shows the comparison of the experimental FRFs at the two mentioned operational conditions, in the frequency range between 2000 and 4000Hz, where the main pump modes occur. The figure clearly shows two peaks at about 2300Hz and 2700Hz corresponding to the first two natural frequencies of the pump. It is interesting to note that the peaks referring to the condition "without oil" occur at major frequencies than the peaks referring to the condition "with oil at 23 bar". This is due to the mass effect that the oil introduces in the system under study. This phenomenon is captured by the developed structural FE model, which includes the effect of the oil as concentrated mass (see also Section 3). The figure also highlights that the amplitude of the FRF is higher in the case "with oil at 23 bar", due to the contribution of the oil in pressure. This phenomenon is not considered by the structural FE model presented above. However, it is very important since the FRF amplitude is increased of about 4 times in correspondence of the peak at 2700Hz (from 6 to 24  $\text{kg}^{-1}$ ), see Figure 4. For this reason, the structural FE model was improved and a coupled vibro-acoustic problem (acoustic and a structural problem) has been solved simultaneously to include the mutual coupling interaction between the fluid pressure and the structural deformation. Figure 5 depicts the cavity mesh developed for the pump being studied, which has been coupled to the structural one for the solution of the vibro-acoustic problem. The cavity mesh has the fluid properties of the pumping oil. In order to verify the effectiveness of the coupled vibro-acoustic FE model with respect to the genuine structural FE model described above, an FRF analysis (SOL 111 in MSC.Nastran driven from LMS Virtual.Lab [8][9]) is carried out with excitation point in C and response point in B, along X' direction. It is worth noting that the damping introduced in this numerical FRF analysis is evaluated by means of the experimental modal analysis performed on the pump at the condition "with oil at 23 bar", see Table 1.

Scenario	Modal damping [%]	Modal damping [%]
	for the 1 <sup>st</sup> mode	for the 2 <sup>nd</sup> mode
Without oil	6	4
With oil at 23 bar	5	0.87

Table 1: Experimental modal damping obtained by modal analysis in different scenarios

On the vibro-acoustic FE model, a forced analysis has been carried out (SOL 111 in MSC.Nastran) with the aim at obtaining the vibration level on the entire pump in operational conditions. The excitations are

the pressure forces and moments and the bearing reactions exchanged between the gears and the casing as well as the variable output pressure of the oil exerted to the pump casing, flange and cover. The LP model gives as outputs the dynamic forces acting on gears that obviously have the same modulus and direction but opposite sense of the forces acting on the casing as shown in Figure 6. These are actually two pressure forces and two bearing forces, concerning the two gears. As an example of these forces, Figure 7 shows the pressure force and bearing reaction of gear 1 along the X' direction at the operational condition of 3000 rpm and 90 bar as a function of frequency. Such forces have peaks in correspondence of the meshing frequency, as expected. In the vibro-acoustic FE model, such forces have been located in the centre of the cavity where the gears are housed, as shown in Figure 6. The LP model can also estimate the variable output pressure. This pressure has been applied to the areas depicted in Figure 8 where actually this pressure acts in operational conditions. The forced analysis has been carried out using excitations estimated by the LP model at the operational condition of 3000 rpm and 90 bar.

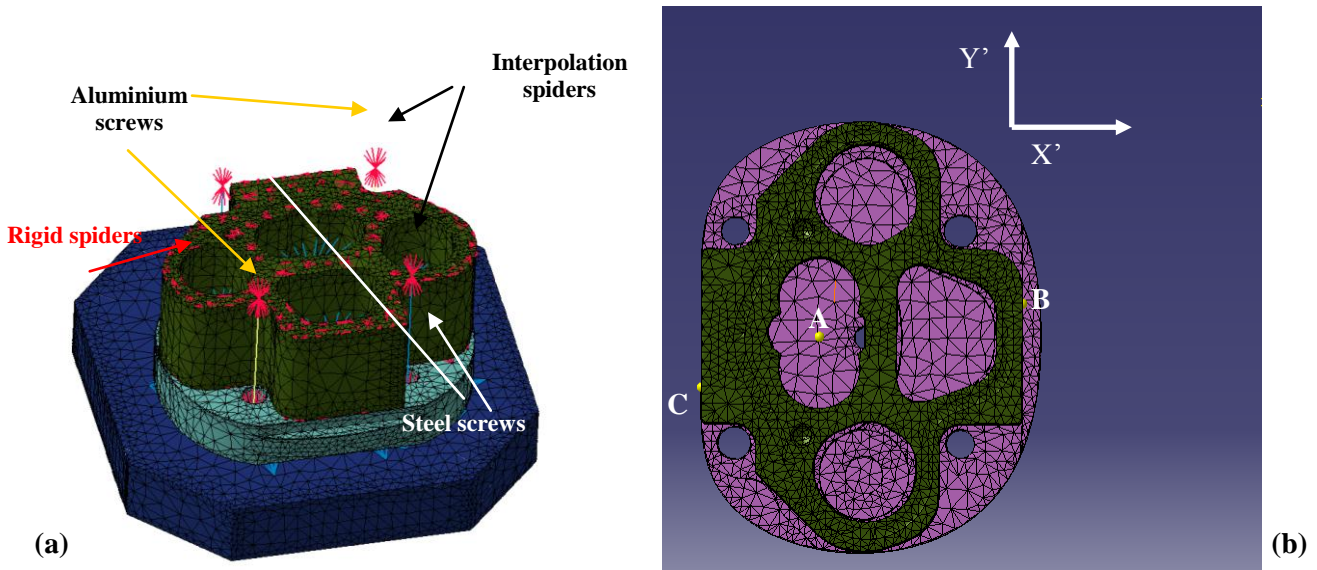


Figure 3: (a) Beam elements modelling the screws (in blue and yellow) and rigid spiders (in red) between case and cover and (b) input and output points set in the FRF analysis

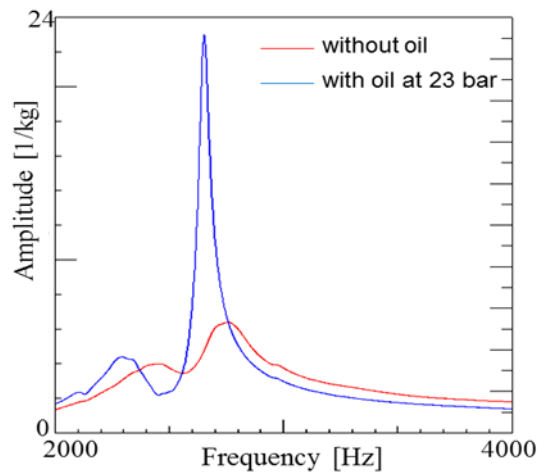


Figure 4: Experimental FRF amplitude for tests without oil and with oil at 23 bar with excitation in C and response in B, along the X' direction

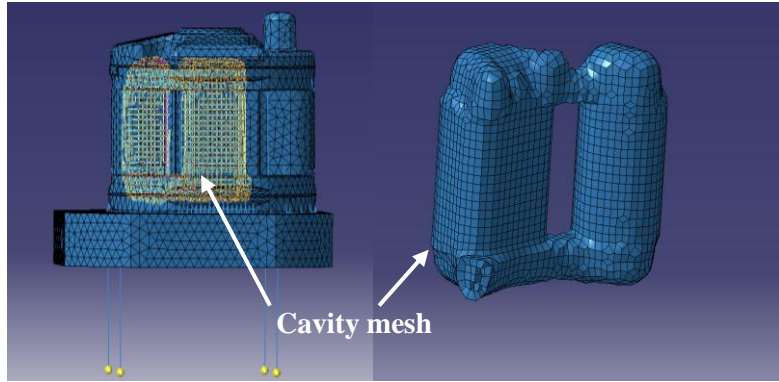


Figure 5: Cavity mesh

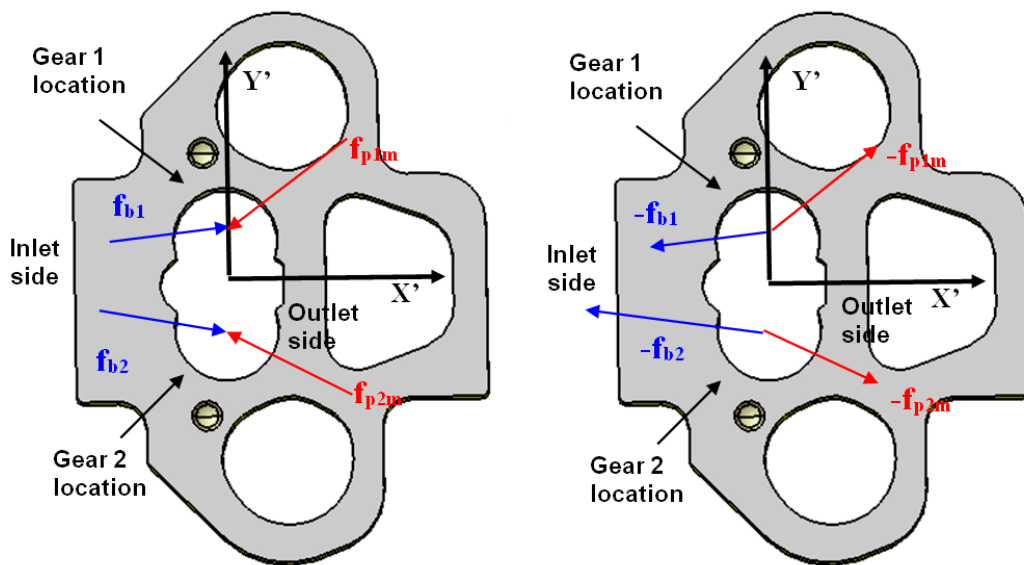


Figure 6: Pressure forces and bearing reactions acting on gears (left) and on the casing (right)

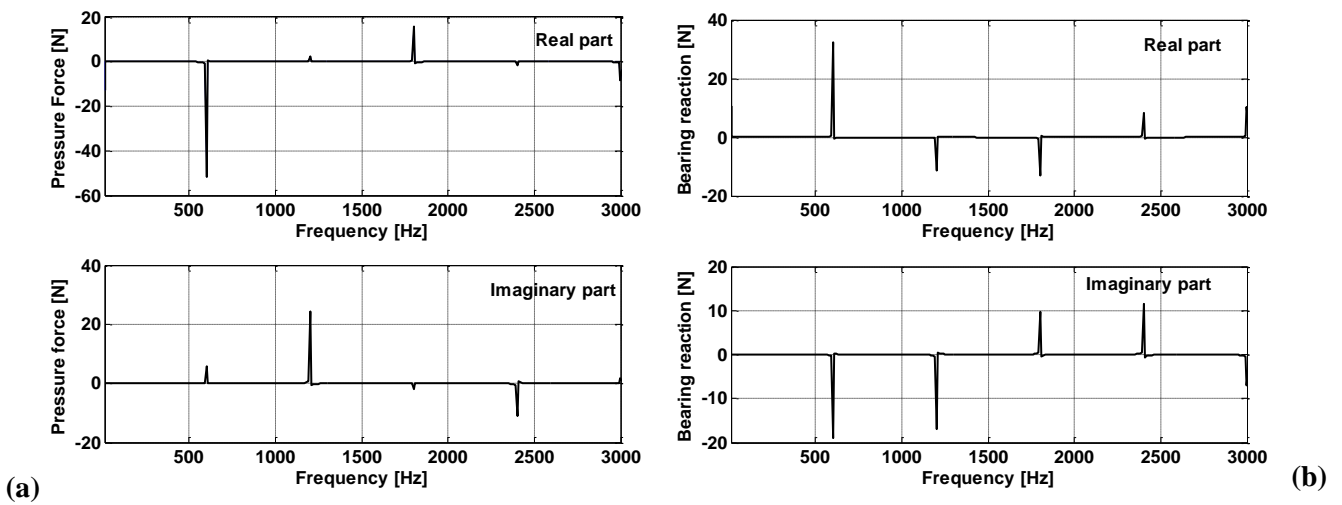


Figure 7: Pressure forces (a) and bearing reactions (b) acting on gear 1 at the operational condition of 3000 rpm and 90 bar

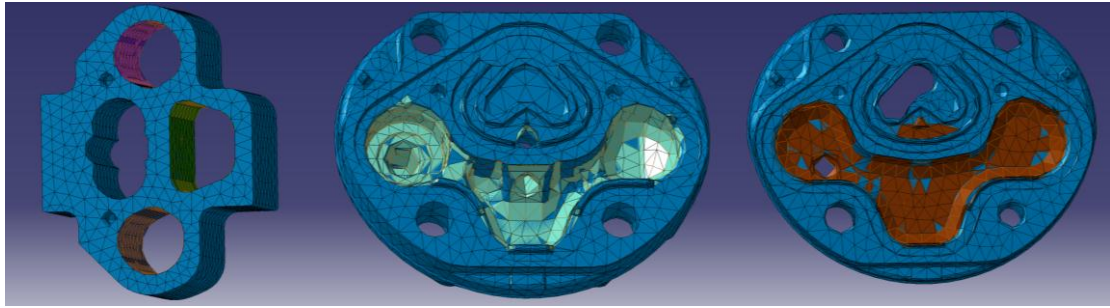


Figure 8: Areas of application of the variable output pressure

### 2.3 Boundary element model simulating noise generation

The vibration level on the pump surface obtained by the forced vibro-acoustic FE analysis has been used as input data for the acoustic simulation in order to determine the noise emitted by the pump in operational conditions. The developed acoustic model should reproduce the acoustic behaviour of test bench in which the pump has been experimentally tested, in order to enable the comparison between experimental and numerical data. The same test bench used for the validation of the LP and FE model has been used hereafter for the acoustic characterization (Figure 2a). Two microphones have been used in order to measure the acoustic pressure in operational conditions, located at a distance of 20 cm from the pump. From an acoustic point of view, the test bench represents a chamber with walls of unknown acoustic impedance. The chamber's walls are sandwich panels of steel and mineral wool. The indirect BE method has been used in order to model such a system, since we are interested in the acoustic pressure field in the exterior of the pump and in the interior of the test bench. By means of the indirect BE method the interior and exterior problem are solved simultaneously. Two output points, B\* and C\* (on the same side as points B and C used during the vibration analysis, respectively) have been located in the same position as the microphones in order to estimate the acoustic pressure to be compared with experiments (see Figure 9a). The test bench walls have been modelled as a box of the same dimension as the real one (see Figure 9b) and characterized by the complex acoustic impedance of the mineral wool (variable in the frequency domain). The acceleration level on the pump casing surface obtained by the previous vibro-acoustic FE analysis (Section 2.2) has been used as input data for the determination of the acoustic pressure inside the box.

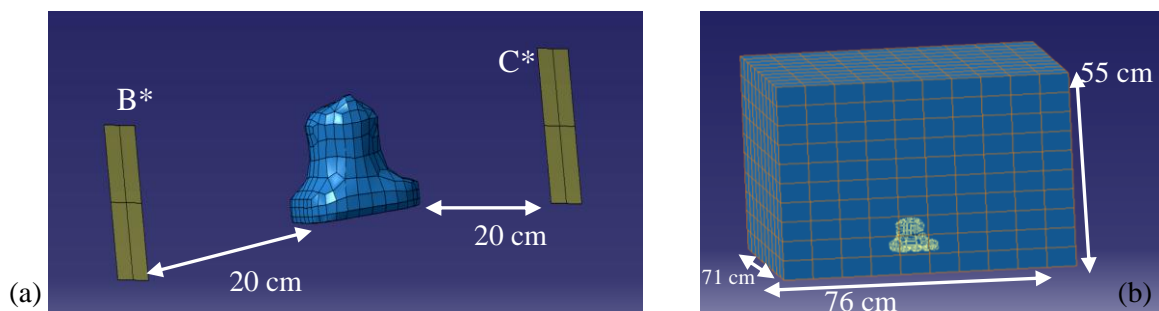


Figure 9: (a) BE model and relative output points (B\* and C\*) and (b) dimension of the box representing the test bench

### 3 Validation results and discussion

Hereafter the results concerning the vibro-acoustic FE model and BE model are compared with experiments. Model results have been obtained by using pump parameters of Table 2.

The numerical FRFs obtained by the vibro-acoustic FE model and the structural FE model are compared with the experimental FRF obtained by hammer and accelerometers (see Section 2.2). Figure 10 depicts such a comparison in the frequency range of interest (2000-3000Hz), where normal modes occur. The amplitude of the vibro-acoustic FRF is similar to the amplitude of the experimental FRF. On the other hand, the structural FRF presents amplitude extremely smaller than the experimental one, as already described in Figure 4. Concerning the frequency contents, Table 3 resumes the first two natural frequencies for the same three scenarios of Figure 10. The numerical natural frequencies are obtained by a modal analysis, SOL 103 in MSC.Nastran driven from LMS Virtual.Lab. The results concerning the structural simulation and the vibro-acoustic simulation are the same in terms of natural frequencies (Table 3). This is due to the fact that both the structural FE model and the vibro-acoustic FE model take into account the oil mass, the first as concentrated mass, while in the second by the mesh. The difference in percentage between the experimental frequencies and the numerical ones is 13% and 5% for the first and second natural frequency, respectively. This difference is also confirmed by the peak location along the horizontal axis in the FRFs of Figure 10.

Value for gear 1	Value for gear 2	Description
$a = 14.65 \text{ mm}$		Centre distance of gear pair
$b_1 = 12.1 \text{ mm}$	$b_2 = b_1$	Gear face width
$E = 210 \cdot 10^9 \text{ Pa}$		Young's modulus
$\nu = 0.3$		Poisson's ratio
$J_1 = 4.0714 \cdot 10^{-7} \text{ kg} \cdot \text{m}^2$	$J_2 = 3.9564 \cdot 10^{-7} \text{ kg} \cdot \text{m}^2$	Moment of inertia
$K_T = 8.053 \cdot 10^2 \text{ Nm/rad}$	-	Torsional stiffness of the driving shaft
$m_1 = 0.0333 \text{ kg}$	$m_2 = 0.0216 \text{ kg}$	Mass
$\hat{m} = 1.150 \text{ mm}$		Gear module
$r_{b1} = 6.484 \text{ mm}$	$r_{b2} = r_{b1}$	Base radius
$\hat{x}_1 = \text{***}$	$\hat{x}_2 = \hat{x}_1$	Addendum modification coefficient (***) confidential
$z_1 = 12$	$z_2 = z_1$	Number of teeth
$\alpha = 20 \text{ deg}$		Pressure angle
$B_{oil} = 1400 \text{ MPa}$		Oil bulk modulus
$\mu = 14 \text{ mPa s}$		Lubricant dynamic viscosity

Table 2: Dimensions and properties of gears

Figure 11a shows the comparison between the experimental and numerical acceleration spectra of the casing surface in correspondence of point B (Figure 3b). The experimental acceleration has been measured by means of piezoelectric accelerometer mounted on point B at the operational condition of 3000 rpm and 90 bar, while the numerical one has been obtained by the forced analysis performed on the vibro-acoustic FE model. The curves show peaks in correspondence of the meshing frequency and relative harmonics as expected. The peaks are amplified by the resonances of the casing, in particular at the frequency around 2400Hz. The comparison between the numerical and experimental curves highlights that the developed



model is able to capture the trend of the experimental curves, even if differences occur, in particular at the meshing frequencies of 2400Hz (3<sup>rd</sup> harmonic) and 3000Hz (4<sup>th</sup> harmonic).

Figure 11b shows the comparison between the experimental and numerical spectra of the acoustic pressure in correspondence of field point B\*. The figure shows the first ten harmonics of the meshing frequency, between 600Hz (1<sup>st</sup> harmonic) and 6000Hz (10<sup>th</sup> harmonic). Differences between numerical and experimental occur in the amplitude of several harmonics (1<sup>st</sup>, 2<sup>nd</sup>, 4<sup>th</sup>, 6<sup>th</sup>, 7<sup>th</sup>) while for others (3<sup>rd</sup>, 5<sup>th</sup>, 10<sup>th</sup>) the correspondence is good. In between the harmonics, the spectra are largely different: this is due to the excitation forces estimated by the LP model, which exist only in correspondence of the meshing frequency and relative harmonics, while they are zero elsewhere. However, this difference does not influence the global acoustic behaviour that is dominated by the highest harmonics peaks. Globally, the pressure level estimated by test is 73.8 dB and it is 74.4 dB when estimated by the model. This means that the model is able to capture the global vibro-acoustic behaviour of the real pump.

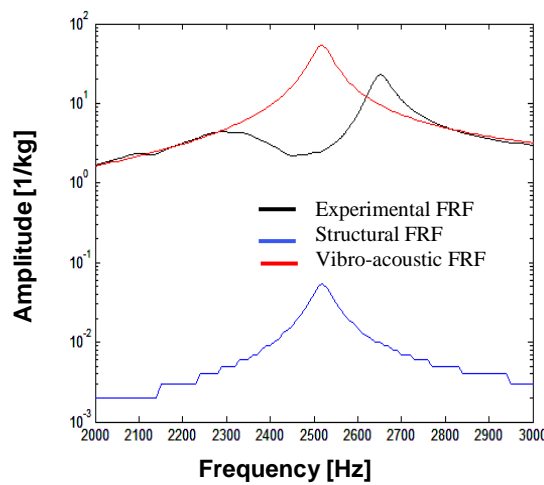


Figure 10: Amplitude of FRFs with excitation in C and response in B, along the X' direction

Mode	Experimental $f_n$ [Hz]	Structural $f_n$ [Hz]	Vibro-acoustic $f_n$ [Hz]
1	2325	2013	2013
2	2651	2518	2518

Table 3: First two natural frequencies obtained from experimental modal analysis, structural FE simulation and vibro-acoustic FE simulation

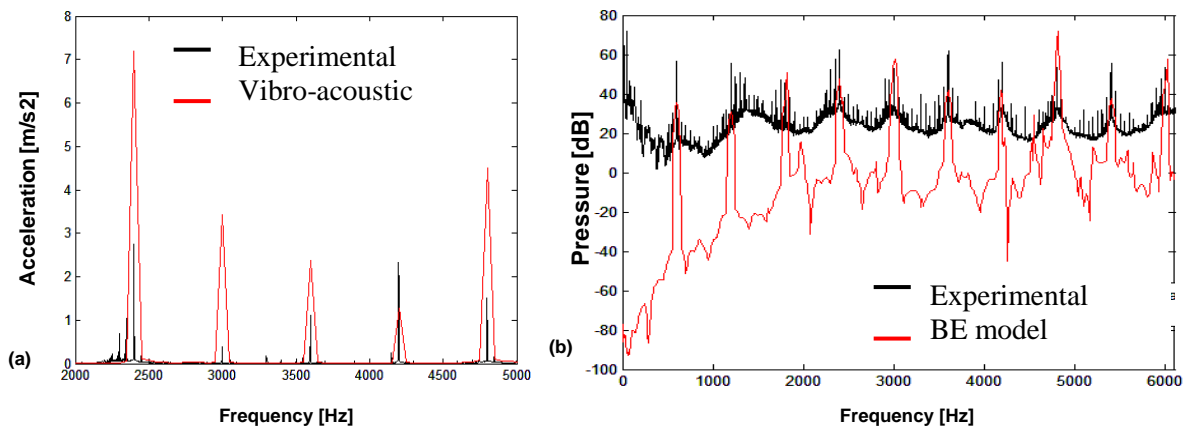


Figure 11: (a) Acceleration spectra in point B at 300rpm and 90 bar and (b) acoustic pressure spectra at location B\*: experimental and simulation results

#### 4 Concluding remarks and further developments

This work addresses the development of a combined LP/FE/BE model for the vibro-acoustic analysis of gear pumps for automotive applications. The lumped-parameter part of the model aims at obtaining the gear accelerations and the forces between the moving parts and the casing, the FE model estimates the external casing accelerations using the excitation forces coming from the LP model; the BE model estimates the noise emitted by the pump in operational conditions. Particular attention has been paid in the inclusion of the oil effect inside the pump casing: the fluid-structure interaction between oil and pump casing has been taken into account. The model has been experimentally assessed. The validation results show that the model is able to foresee system resonances and to estimate the amplitude of the vibrations on the external surfaces of the pump as a function of working conditions as well as the emitted noise. This model could be a very useful tool in prototype development and in design optimisation in order to identify the origin of unwanted dynamic effects. However differences between numerical and experimental data still exist.

In order to improve the accuracy of the simulation results and therefore in order to achieve a behaviour closer to the real measurements, the model should be further developed. In particular, in the forced analysis of the vibro-acoustic FE model, damping has been introduced as modal damping estimated by an experimental modal analysis (EMA). This EMA was performed on the pump at the condition “with oil at 23 bar”, in which the 23 bar pressure has been obtained by an external equipment. On the contrary the vibro-acoustic FE forced analysis has been carried out at the output pressure of 90 bar. It has been demonstrated that the modal damping is very sensitive to the output pressure. Table 1 collects the modal damping values obtained by an experimental modal analysis at two different conditions: “without oil” and “with oil at 23 bar”. The difference is large in particular for the 2<sup>nd</sup> mode, as also depicted in Figure 4. Therefore, it is expected that the modal damping is different for a pressure of 90 bar. Further investigations have to be carried out about this aspect, in order to estimate the modal damping corresponding to 90 bar of output pressure and include its in the numerical forced analysis. Furthermore, the effective acoustical impedance of the test bench walls has to be experimentally determined.

## Acknowledgements

This work has been developed within the Advanced Mechanics Laboratory (MechLav) of Ferrara Technopole, realized through the contribution of Regione Emilia-Romagna - Assessorato Attività Produttive, Sviluppo Economico, Piano telematico – *POR-FESR 2007-2013*, Activity I.1.1.

## References

- [1] E. Mucchi, G. Dalpiaz, A. Fernández del Rincón, *Elasto-dynamic analysis of a gear pump. Part I: pressure distribution and gear eccentricity*, Mechanical Systems and Signal Processing, Vol. 24 (2010), pp. 2160-2179.
- [2] E. Mucchi, G. Dalpiaz, A. Rivola, *Elasto-dynamic analysis of a gear pump. Part II: meshing phenomena and simulation results*, Mechanical Systems and Signal Processing Vol. 24 (2010), pp. 2180-2197.
- [3] E. Mucchi, G. Dalpiaz, A. Rivola, *Dynamic behaviour of gear pumps: effect of variations in operational and design parameters*, Meccanica Vol. 46, No. 6 (2011), Page 1191-1212.
- [4] B. Zardin, F. Paltrinieri, M. Borghi, M. Milani, *About the prediction of pressure variation in the inter-teeth volumes of external gear pumps*, in: Proceedings of the 3rd FPNI-PhD Symposium on Fluid Power, Spain, 2004.
- [5] C. Bonacini, M. Borghi, *Calcolo delle pressioni nei vani fra i denti di una macchina oleodinamica ad ingranaggi esterni*, Oleodinamica-pneumatica, 1991 (in Italian).
- [6] D. Childs, H. Moes, H. Van Leeuwen, *Journal bearing impedance descriptions for rotordynamic application*, Journal of lubrication technology, 99 (1977) 198-214.
- [7] G. Dalpiaz, A. Fernández del Rincón, E. Mucchi, A. Rivola, *Experimental validation of a model for the dynamic analysis of gear pumps*, Proceedings of Novem 2005, Saint Raphael, France, 2005.
- [8] MSC, MSC.NASTRAN, Version 2011, 2011.
- [9] LMS International, LMS Virtual.Lab, 2011.

